

# Thermal Comptonization in GRS 1915+105

Osmi Vilhu

Observatory, Box 14, FIN-00014 University of Helsinki, Finland

osmi.vilhu@helsinki.fi

Petter Nikula

Observatory, Box 14, FIN-00014 University of Helsinki, Finland

petter.nikula@helsinki.fi

Juri Poutanen

Stockholm Observatory, SE-133 36 Saltsjöbaden, Sweden

juri@astro.su.se

and

Jukka Nevalainen

ESA/ESTEC Astrophysics Division, Box 299, 2200 AG Noordwijk, The Netherlands

jnevalai@astro.estec.esa.nl

Received ;;    accepted :

## ABSTRACT

The Rossi X-ray Timing Explorer (*RXTE*) data of GRS 1915+105 from several observing periods were modelled with a thermal Comptonization model. In the model, seed soft photons from an optically thick cool disk are Comptonized in a hot spherical corona surrounding the inner disk. Best fit models indicate that there are strong correlations between the inner disk temperature, the disk luminosity and the ratio of the inner radius to the coronal one ( $R_{in}/R_{cor}$ ). The spectral hardness of the Comptonized radiation, quantified by the Kompaneets  $y$ -parameter, anti-correlates with the disk luminosity. The inner disk - coronal interface was small ( $R_{in}/R_{cor} = 1$ ) at high and moderate luminosity states and increased non-linearly to  $R_{in}/R_{cor} \leq 0.8$  towards lower luminosities. The sensitivity of the disk luminosity on  $R_{in}/R_{cor}$  at high (and soft) states may be the reason for the observed rich pattern of variability. However, deviations from the general trend can be expected during some peculiar states (e.g. during rapid inner disk removals or hard-steady radio loud states).

*Subject headings:* accretion, accretion disks – binaries: close – black hole physics – instabilities – stars: individual (GRS 1915+105) – X-rays: stars

## 1. Introduction

The X-ray transient GRS 1915+105 was discovered by Castro-Tirado et al. (1992) using WATCH all-sky monitor on the GRANAT satellite. Since then it has been one of the most luminous X-ray sources in the sky. Mirabel and Rodriquez (1994) found first Galactic superluminal radio-jets (multiple ejections of plasma clouds) at an angle of  $70^{\circ}$  to the line of sight in this Galactic black hole candidate which lies at a kinematic distance of  $12 \pm 1.5$  kpc (Chaty et al. (1996), Fender et al. (1999)).

The *Rossi X-ray Timing Explorer (RXTE)* has been monitoring it frequently and a rich pattern of variability has emerged from these data with time scales from years down to 15 msec (Greiner et al. (1996), Chen et al. (1997), Morgan et al. (1997), Taam et al. (1997), Belloni et al. (1997a), Belloni et al. (1997b), Vilhu and Nevalainen (1998), Trudolyubov et al. (1999), Markwardt et al. (1999), Munro et al. (1999), Belloni et al. (2000)). The overall spectral shape in the 2 - 50 keV energy range has been modelled with an absorbed disk black body accompanied by a power law component (see e.g. Trudolyubov et al. (1999), Markwardt et al. (1999), Munro et al. (1999)).

Vilhu and Nevalainen (1998) used a 2-phase thermal Comptonization model in which the disk penetrates into the central coronal region where the Comptonization of disk photons takes place. This geometry is similar to that of the advection dominated accretion flow (ADAF) (see e.g. Esin et al. (1997)) but is not a unique one (see, e.g. Poutanen (1998)). In the present paper, such a thermal Comptonization model is applied for RXTE data of GRS 1915+105 (PCA and HEXTE instruments) collected from several observing intervals during 1996-1997.

## 2. Observations

We collected 36 Proportional Counter Array (PCA) and High-Energy X-ray Timing Experiment (HEXTE) observations of GRS 1915+105, performed during 1996-97, from the TOO-archive of *RXTE*, with typical observing times of a few hours. Figure 1 shows the ASM (*RXTE* All Sky Monitor) light curve with the selected PCA and HEXTE observations marked. The Standard-2 data with 128 (PCA) and 64 (HEXTE) channels of spectral information and 16 sec temporal resolution were used. All five PCU's (proportional counter units) and both HEXTE clusters were used. The background was subtracted although its effect was not crucial, since we limited the PCA- and HEXTE-spectra in the range 2-25 keV and 15-60 keV, respectively.

Inside each of the 36 observation periods, the data were binned into separate luminosity groups (1 - 5) to accumulate a spectrum, resulting in 101 individual spectra. Figure 2 shows the spectra in the 2-colour diagramme. 'LULL' refers to the long minimum phase in the middle of Fig.1, while 'UPS' and 'DOWNS' mark the approximate positions of maxima and minima in the strongly oscillating light curve analysed by Belloni et al. (1997a) (obsid 20402-01-33-00). The letters A, B and C show the locations of the three main variability types found by Belloni et al. (2000).

EDITOR: PLACE FIGURE 1 HERE.

EDITOR: PLACE FIGURE 2 HERE.

### 3. Model

In the model, the disk penetrates into the central spherical coronal region with electron temperature  $kT_e$ , Thompson optical depth  $\tau$  and coronal radius  $R_{cor}$ . The optically thick multi-temperature disk, with inner disk radius  $R_{in}$ , radiates the observed soft spectrum and serves as the source of seed photons for Comptonization in the corona. No other sources of soft (e.g. synchrotron) photons were assumed.

A fraction of the disk photons penetrates into the corona and experience (before escaping) multiple Compton scatterings building the hard part of the observed spectrum where the reflection component (from the disk) is also included. The radiative transfer in the corona was handled by the iterative scattering method developed by Poutanen & Svensson (1996) and incorporated into the XSPEC spectral fitting software of the XANADU package (see Poutanen (1998), Vilhu et al. (1997)). The model is physically self-consistent and predicts the normalization between the soft and hard components, as well as the power-law photon index.

The temperature-stratification of the disk in the radial-direction is that of the classical viscous disk  $T(r) = T_{in}(r/R_{cor})^{-3/4}$ , and assuming a constant temperature  $T(r) = T_{in}$  inside the coronal region (between  $R_{in}$  and  $R_{cor}$ ). The local spectrum was assumed to be a black body and the integration over the disk gave the total disk-spectrum (Frank et al. (1992)).

To obtain both the coronal temperature and optical depth of GRS 1915+105 is beyond the RXTE capability. However, the Kompaneets  $y$ -parameter ( $y = 4\tau\Theta$  where  $\Theta = kT_e/m_e c^2$ ) is rather well constrained in the model. We fixed  $kT_e$  at 70 keV and fitted  $y$ , but made numerous fits also with  $kT_e = 30$  keV and 150 keV. The  $y$ -parameter determines mainly the hard spectral slope (the photon index) while the ratio of the inner disk and coronal radii ( $R_{in}/R_{cor}$ ) controls the fraction of seed disk photons entering the corona, and consequently the hard/soft ratio. The inclination  $70^\circ$  was used, assuming that the jets are

perpendicular to the disk (Mirabel and Rodriquez (1994)).

It turned out that by letting the three parameters  $T_{in}$ ,  $y$  and  $R_{in}/R_{cor}$  to vary (and fixing the inclination, Hydrogen column density  $N_H$  and  $kT_e$ ), all PCA/HEXTE spectra of GRS 1915+105 can be fitted with the model.

#### 4. Results

The PCA/HEXTE spectra were fitted with the above ('Sombrero') model and XSPEC-software allowing a systematic error 0.02 and achieving reduced  $\chi^2$ -values less than 1.2. Figure 3 shows the fitting results as a function of the disk luminosity  $L_{\text{disk}}$  (assuming distance 12.5 kpc). The power-law photon index (determined by power law fits) is also shown in the panel Fig.3e and can be approximated by photon index =  $2.0 + 0.2y^{-1}$ , where  $y$  is the Kompaneets-parameter shown in Fig.3b.

EDITOR: PLACE FIGURE 3 HERE.

Models using a power law overestimate the low energy part of the hard component, while in the Comptonized models there is a stronger low energy cut-off in that component (see Figures 4 and 5).

EDITOR: PLACE FIGURE 4 HERE.

EDITOR: PLACE FIGURE 5 HERE.

This fact leads to a smaller  $N_H$  and a larger  $T_{in}$  (as compared with the power law fits), especially during the low luminosity phases where the relative role of the hard component

is large (the ratio  $L_{\text{hard}}/L_{\text{disk}}$  strongly increases with decreasing  $L_{\text{disk}}$ , see Fig.3f). We run fit-statistic contour plots between  $N_H$  and  $T_{in}$  for several spectra and found a small systematic trend of increasing  $N_H$  with  $T_{in}$  but fixed  $N_H$  at  $2.3 \times 10^{22} \text{ cm}^{-2}$ . This value is close to the Galactic neutral Hydrogen column  $2 \times 10^{22} \text{ cm}^{-2}$  in the direction of GRS 1915+105 (Dickey and Lockman (1990)).

The inner disk temperature  $T_{in}$ , the coronal  $y$ -parameter and  $R_{in}/R_{cor}$  strongly correlate with the disk luminosity (Figs.3a-c), while the hard Comptonized luminosity (Fig.3f) is relatively constant, leading to a strongly increasing hard/disk ratio with decreasing  $L_{\text{disk}}$ . The inner disk radius (Fig.3d) is also quite constant (25 - 40 km without relativistic and colour corrections), in particular the radii during high and low states do not differ appreciably. However, in some observations with rapid violent changes, the inner radius increased during 'DOWNS' to 60 km and this was interpreted by Belloni et al. (1997b) as due to rapid disappearance of the inner disk annulus into the underlying black hole. This particular observation (obsid 20402-01-33-00) was divided into 5 count rate classes and 'UPS' and 'DOWNS' refer to the highest and smallest count rate spectra, respectively.

The choice of  $kT_e$  has some effect on  $R_{in}/R_{cor}$  as shown by the dash-dot lines in Fig.3c giving systematic differences when  $kT_e$  is selected between 30 - 150 keV. The functional dependence between  $L_{\text{hard}}/L_{\text{disk}}$ ,  $R_{in}/R_{cor}$  and  $kT_e$  is complex but can be rather well approximated by  $x/T_{70} = \exp(5(\sqrt{L_{\text{hard}}/L_{\text{disk}}}-1))$  where  $x = 1 - R_{in}/R_{cor}$  and  $T_{70}$  is the coronal temperature in units of 70 keV.

## 5. Discussion

The mass accretion rates were high amounting to  $(0.1 - 1.5) \times \dot{M}_{Edd}$  (for a  $10M_{\odot}$  black hole) where  $\dot{M}_{Edd} = 10L_{Edd}/c^2 = 1.39 \times 10^{18} M/M_{\odot} \text{ g s}^{-1}$  corresponds to a radiative efficiency of 0.1. The inner disk radius lies in a rather narrow range of 25 - 40 km if the sudden removals of the inner disk annulii are removed ('DOWNS' in Fig.3d). The high and low state radii do not differ considerably. This result is different from that using a power law model which requires smaller  $T_{in}$  at low luminosity and hard states. On the other hand, the Kompaneets y-parameters and the Comptonized fraction (as measured by  $R_{in}/R_{cor}$ ) deviate significantly between these two extreme states (see Figs. 3b and 3c).

One should be cautious with the absolute  $R_{in}$ -values derived, since relativistic and color corrections can be large. Using the results by Zhang et al. (1997) at inclination  $70^{\circ}$ , one obtains the factors 1.23 and 1.07 for a non-rotating and an extreme prograde Kerr hole, respectively, by which the radii in Fig.3d should be multiplied to obtain the innermost radius of the disk. After these corrections the mass of GRS 1915+105 should be smaller than  $4M_{\odot}$  and  $22M_{\odot}$  for a non-rotating and an extreme prograde Kerr hole, if the average radius derived (30 km in Fig.3d) equals to the last marginally stable orbit ( $3r_g$  and  $0.5r_g$  for non-rotating and Kerr hole, respectively).

Perhaps the most important property emerging from the present modelling is the strong dependence of the disk luminosity on the disk-corona interface (the region from  $r = R_{in}$  to  $r = R_{cor}$ , see Fig.3c). This conclusion remains valid even if there are systematic differences between the coronal temperatures of low/hard and high/soft states (see the dot-dashed lines in Fig. 3c). A further support is given by the existence of a reflection component in the low state spectra (included in the model), while during high states the reflection was found to be very small.

The instability of the system (large observed bewildering variabilities at high



luminosity states) may be due to the extreme sensitivity on  $R_{in}/R_{cor}$  when this parameter is close to 1 (see Fig. 3c). This interface region may also be the site for the 2 - 10 Hz QPO's, their locations are marked in Fig.3e just for reference as estimated from Trudolyubov et al. (1999) and Munro et al. (1999). When the inner disk penetrates more and more into the corona ( $R_{in}/R_{cor}$  decreases and the  $y$ -parameter and coronal mass increase), intuitively one expects the QPO-amplitude to increase (and frequency to decrease) as observed.

Although the general trend (as a function of luminosity) can be explained with the present model between 2 - 60 keV, non-thermal processes (to explain the hard tail observed by OSSE/CGRO) are certainly important during some phases (Vilhu et al. (1999), Hannikainen et al. (1999b), Poutanen (1998), Coppi (1999)). Further, as already remarked above in the case of 'DOWNS', some peculiar states may significantly deviate from the general trend. Such interesting states are e.g. the radio-loud hard-steady states (the small lulls in Fig.1 at JD 2450290 and 2450730) after which radio-flares or superluminal jet-ejections were observed (see e.g. Hannikainen et al. (1999a), Hannikainen (1999c)). They are not included in our data-set but power law fits (Munro et al. (1999)) indicate that they deviate from the hard-steady radio quiet state (the 'LULL' in Fig.1) by having a very hot inner disk with a small radius.

## 6. Conclusions

Rossi XTE data (PCA + HEXTE) of GRS 1915+105 in a broad luminosity range ( $2-30 \times 10^{38}$  erg/s) can be modelled with a thermal Comptonization model where seed photons from an optically thick disk are up-scattered in a spherical corona surrounding the inner disk. The inner disk temperature correlates and the Kompaneets  $y$ -parameter anticorrelates strongly with the disk luminosity, while the inner radius and the hard Comptonized luminosity do not depend significantly on the luminosity state (see Figs.3a,b,d,f).

Although both the electron temperature and optical depth of the corona can not be determined separately (only their product via the  $y$ -parameter is well constrained), we conclude that at high soft states the inner disk just touches the outer edge of the hot central corona ( $R_{in}/R_{cor} = 1$ ), while during low hard states the corona is larger and denser and totally surrounds the inner disk ( $R_{in}/R_{cor} \leq 0.8$ , see Fig. 3c).

These results describe the general trend as a function of luminosity, but significant deviations can be expected during some peculiar states (e.g. sudden removals of the inner disk annuli or hard-steady radio loud states).

This research has been supported by the Academy of Finland (OV) and the Swedish Natural Science Research Council and the Anna-Greta and Holger Crafoord Fund (JP).

## REFERENCES

- Belloni, T., Mendez, M., King, A. R., van der Klis, M., & van Paradijs, J. 1997a, ApJ, 479, L145
- Belloni, T., Mendez, M., King, A. R., van der Klis, M., & van Paradijs, J. 1997b, ApJ, 488, L109
- Belloni, T., Klein-Volt, M., Mendez, M., van der Klis, M., & van Paradijs, J. 2000, AA, 355, 271
- Castro-Tirado, A. J., Brandt, S., & Lund, N. 1992, IAU Circ. 5590
- Chaty, S., Mirabel, I. F., Duc, P. A., Wink, J. E., & Rodriguez, L. F. 1996, AA, 310, 825
- Chen, X., Swank, J. H., & Taam, R. E. 1997, ApJ, 477, L41
- Coppi, P. S. 1999, in ASP Conf. Ser. 161, High Energy Processes in Accreting Black Holes, ed. J. Poutanen, R. Svensson (San Francisco: ASP), 375
- Dickey, J., & Lockman, F. 1990, ARA&A, 28, 215
- Esin, A. A., McClintock, J. E., & Narayan, R. 1997, ApJ, 489, 865
- Fender, R. P., Garrington, S. T., McKay, D. J., Muxlow, T. W. B., Pooley, G. G., Spencer, R. E., Stirling, A. M., & Waltman, E. B. 1999, MNRAS, 304, 865
- Frank, J., King, A., & Raine, D. 1992, Accretion Power in Astrophysics, 2nd ed., Cambridge Univ. Press
- Greiner, J., Morgan, E., & Remillard, R. A. 1996, ApJ, 473, L107
- Hannikainen, D. C., Vilhu, O., Alha, L., Hunstead, R. W., & Campbell-Wilson, D. 1999a, in 5th Compton Symposium, in press

- Hannikainen, D. C., Hunstead R. W., Vilhu, O., Campbell-Wilson, D., & Williamson, M. 1999b, in ASP Conf. Ser. 161, High Energy Processes in Accreting Black Holes, ed. J. Poutanen, R. Svensson (San Francisco: ASP), 88
- Hannikainen D. 1999, PhD Thesis, Univ. of Helsinki, ISSN 1455-4852.
- Markwardt, C. B., Swank, J. H., & Taam, R. E. 1999, ApJ, 513, L37
- Mirabel, I. F., & Rodriguez, L. F. 1994, Nature, 371, 46
- Morgan, E., Remillard, R.A., & Greiner, J. 1997, ApJ, 482, 993
- Muno, M. P., Morgan, E. H., & Remillard, R. A. 1999, ApJ, 527, 321
- Poutanen, J., & Svensson, R. 1996, ApJ, 470, 249
- Poutanen, J. 1998, in Theory of Black Hole Accretion Disks, ed. M. A. Abramowicz, G. Björnsson, & J. E. Pringle (Cambridge: Cambridge Univ. Press), 100
- Taam, R. E., Chen, X., & Swank, J. H. 1997, ApJ, 485, L83
- Trudolyubov, S., Churazov, E., & Gilfanov, M. 1999, AA, 351, L15
- Vilhu, O., Nevalainen, J., Poutanen, J., Gilfanov, M., Durouchoux, Ph., Vargas, M., Narayan, R., & Esin, A. 1997, in AIP Conference Proceedings 410, Proceedings of the Fourth Compton Symposium, ed. C. D. Dermer, M. S. Strickman, & J. D. Kurfess (AIP: New York), 887
- Vilhu, O., & Nevalainen, J. 1998, ApJ, 508, L89.
- Vilhu, O., Alha, L., Malmivaara K., Huovelin, J., Poutanen, J., & Nevalainen, J. 1999, Astroph. Letters and Comm., 38, 237
- Zhang, S. N., Cui, W., & Chen, W. 1997, ApJ, 482, L155

Fig. 1.— The ASM light curve (2 - 13 keV) of GRS 1915+105 with the PCA/HEXTE observations used marked with short vertical lines.

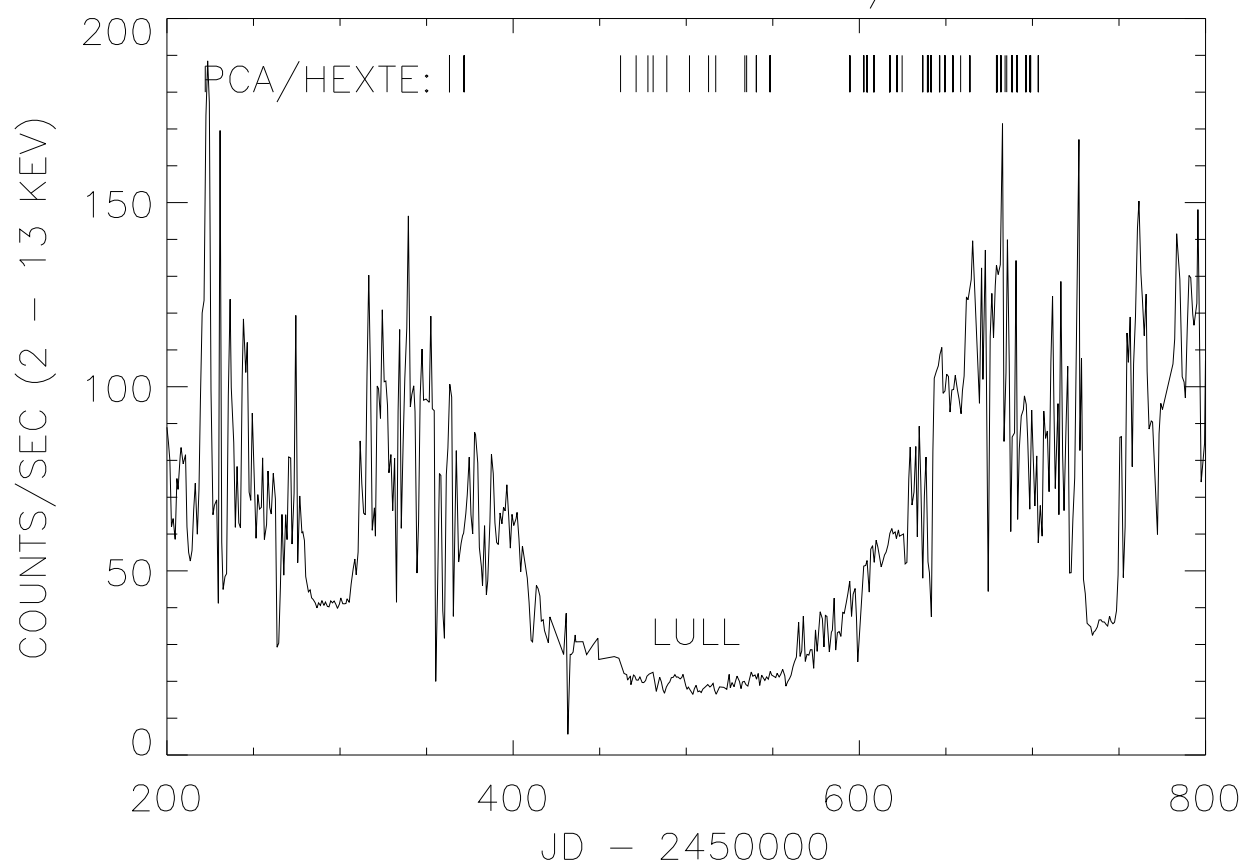
Fig. 2.— The color-color diagram of our set of observations.

Fig. 3.— The results of fitting as a function of the disk luminosity. The coronal temperature was fixed to  $T_e = 70$  keV but the dash-dot lines in panel c show the systematic effect when  $T_e = 30$  keV (upper) and  $T_e = 150$  keV (lower).

Fig. 4.— PCA and HEXTE spectrum from the 'LULL-phase' (obsid 20402-01-16-00) showing also the hard model component and power law fit (solid lines).

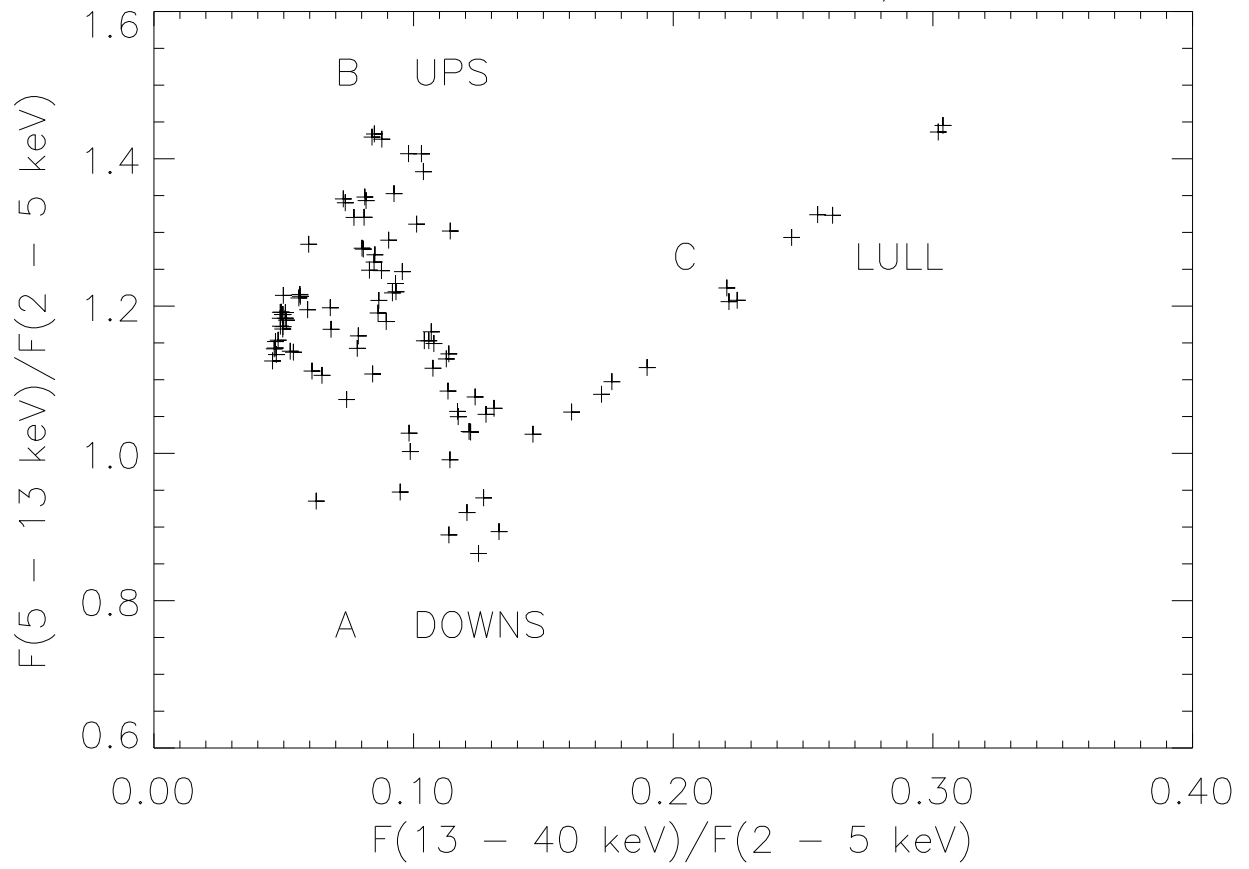
Fig. 5.— PCA and HEXTE spectrum from the 'HIGH-phase' (obsid 20402-01-33-00) showing also the hard model component and power law fit (solid lines).

# GRS 1915+105 RXTE/ASM





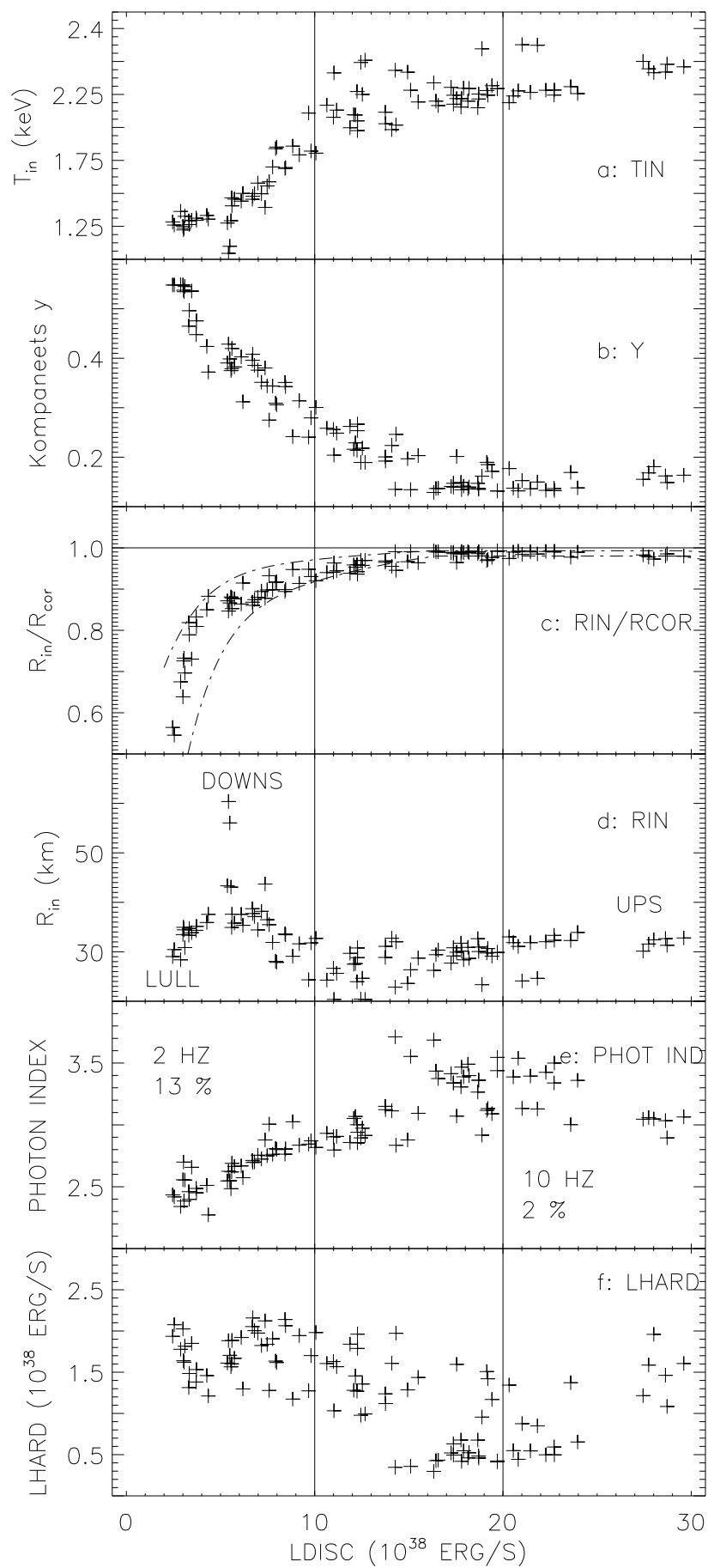
GRS 1915+105 RXTE/PCA



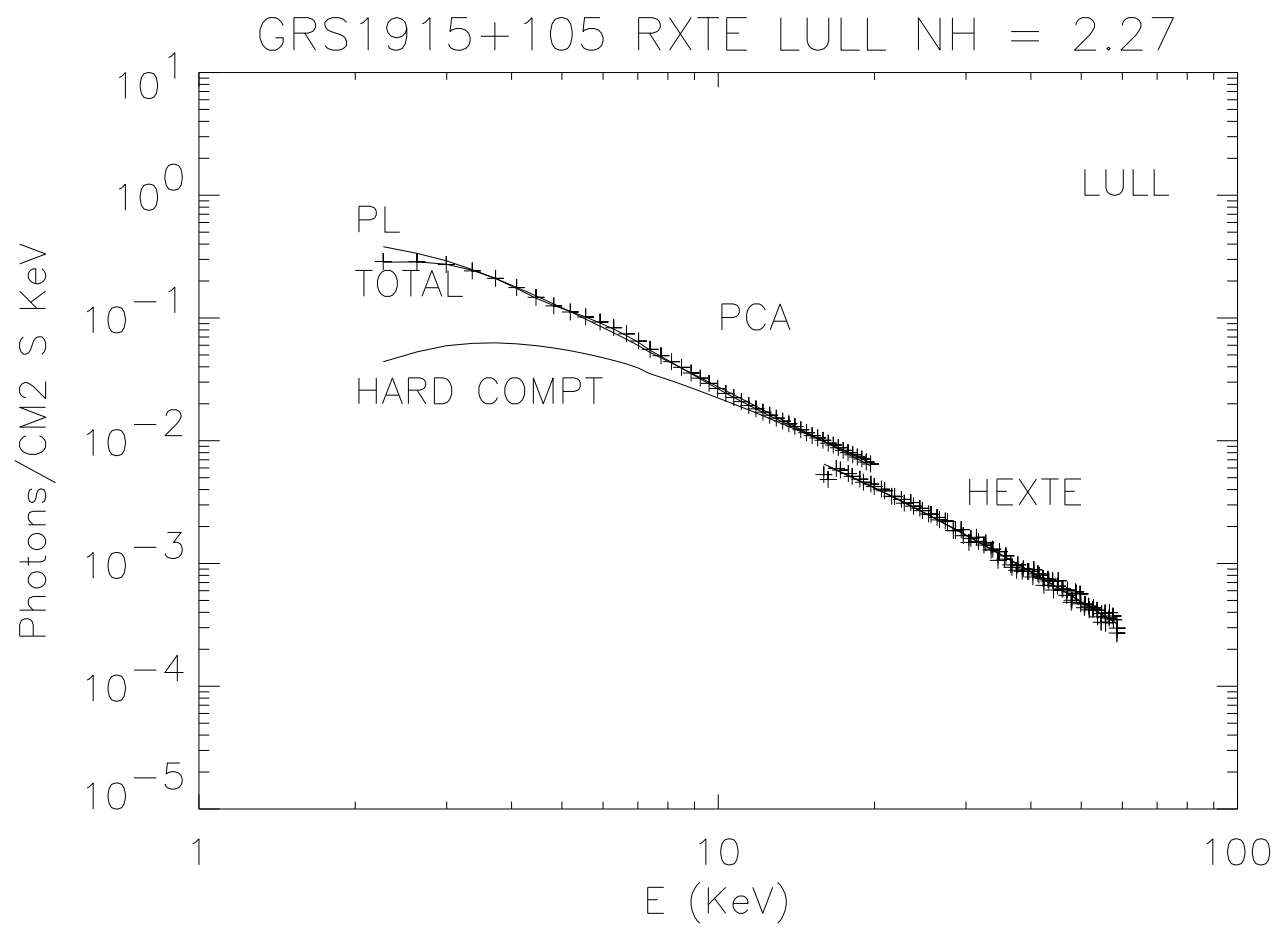




GRS 1915+105 SOMBRERO  $T_e = 70$  keV









GRS1915+105 RXTE HIGH NH = 2.27

